Seismic fragility analysis of multi-span continuous beam bridge considering spatial variation of ground motions

D. Wang[(1)], X. Wang[(2)], H. Liu[(3)]

[(1)] *Associate Professor, School of Civil Engineering & Mechanics, Yanshan University, wangding@ysu.edu.cn*
[(2)] *M. S. Candidate, School of Civil Engineering & Mechanics, Yanshan University, 985138176@qq.com*
[(3)] *M. S. Candidate, School of Civil Engineering & Mechanics, Yanshan University, 18712763752@163.com*

Abstract

Because of good integrity, high structural rigidity and smooth deformation curve, which are all conducive to high-speed driving, continuous beam bridge has been widely used in highway and railway transportation. With increase of span, the effect of the spatial variation of ground motions on the nonlinear response of long-span continuous beam bridge becomes obvious and must be considered. This paper focuses on the effect of the spatial variation of ground motions on the seismic fragility curves of a multi-span continuous beam bridge. Firstly, the finite element model of the continuous beam bridge is established by using OpenSees. After that, based on the models of the evolutionary power spectral density and lagged coherency of nonstationary seismic field, the spectral representation method is used to simulate the uniform and the spatially variable seismic ground motion time histories. The responses of the continuous beam bridge are calculated in these two types of ground motion excitation. Taking the peak acceleration of ground motion (PGA) as the ground motion intensity index and using the linear fitting method based on probabilistic seismic demand analysis (PSDA), the fragility curves of the bridge under the uniform and the spatially variable ground motions are obtained respectively. The analysis result indicates that the multi-span continuous beam bridge is obviously affected by the spatial variation of seismic ground motion, and it is more likely to cause structural failure under uniform excitation.

Keywords: spatial variation of seismic ground motions; fragility analysis; multi-span continuous beam bridge; seismic response; ground motion simulation

1. Introduction

China is one of the countries with the most serious seismic disasters in the world. Seismic risk evaluation and structural performance assessment have always been heated topics in China. The performance-based probabilistic decision framework proposed by the Pacific Earthquake Engineering Research Center divides the seismic performance assessment of structures into three parts: seismic risk analysis, seismic fragility analysis and seismic loss analysis. Among them, seismic fragility analysis is a core content of seismic probabilistic safety assessment theory [1]. From the perspective of probability theory, seismic vulnerability reflects the relationship between ground motion intensity and the exceeding probability of a particular damage state, which has become an important tool to measure the seismic performance of a structure, and can determine structural weak links [2]. Many studies have been carried out on the vulnerability of bridges. It was indicated that the damage degree of multi-point excitation was larger than that of consistent excitation. Basöz and Kiremidjian identified structural characteristics that were highly correlated with the observed damage of bridge [3] and used logistic regression analysis to establish empirical vulnerability curves [4]. Shinozuka *et al.* assumed that the empirical fragility curve of bridge obeyed the normal distribution and established the empirical fragility curve of the piers of a actual bridge [5]. Further, Shinozuka *et al.* used the fragility curve to study the effect of spatial variation of seismic ground motions on bridge response [6]. Monti *et al.* proposed a simplified probabilistic approach to assess the damage state of an existing bridge in earthquake to determine its current level of safety and ultimately the need for increased intervention [7]. Karim and Yamazaki used the lognormal distribution model of the damage index and the ground motion parameters o constructed brittle curves for four piers of bridge [8]. Elnashait *et al.* used adaptive inelastic dynamic analysis technique to analyze and deduce the fragility function of reinforced concrete Bridge [9]. Lehman *et al.* presented a framework to assess the seismic performance of well-sealed RC bridge columns with circular sections under a range of damage conditions [10]. Jeong and Elnashai proposed an exact solution for a generalized single-degree of-freedom system and used it to build a coefficient response database describing the relationship between logarithmic normal brittleness in common use [11]. The results indicated that the spatial variation of ground motions would not only have a significant impact on the internal force of the bridge structure, but also significantly increase the probability of collision. The research of Liao *et al.* shows that the internal forces of beams and piers of the continuous rigid frame bridge with high pier and long span are greatly affected by the spatial variation of ground motions[12]. Li *et al.* used the displacement ductility ratio of piers to represent the failure state of the bridge and established the vulnerability curve [13]. Han *et al.* used incremental dynamic method to define the failure state of components, and presented the fragility curve of bridge piers and supports by regression analysis [14]. Li and Hao used randomly generated seismic waves to analyze the vulnerability of offshore Bridges [15]. Li *et al.* introduced Nataf transformation in the seismic vulnerability analysis of bridge considering the correlation of random variables [16]. Considering the chloride ion erosion of offshore bridges, Liu and Ren obtained the seismic fragility curve of a bridge and its components based on Monte Carlo method [17]. Kang *et al.* considered the traveling wave effect and the local site effect, and took a typical high-pier railway bridge as an example to conduct a comparative analysis of the collision response [18].

Continuous beam bridges have good mechanical properties, good integrity, large structural stiffness and smooth deformation curve, which are conducive to high-speed driving. They are widely used in highway and railway traffic. At present, the span of pre-stressed concrete continuous beam bridge has reached 150m. Due to the large span, the phase, frequency and intensity of seismic ground motions at each pier will be different, so the spatial variation effect of ground motions should be considered [19]. Spatial variation effect of ground motions includes coherence effect, traveling wave effect, attenuation effect, site effect, etc.[20]. The spatial variation of ground motions has significant effect on the seismic nonlinear response of long-span bridge. However, there are few seismic fragility analyses of continuous beam bridges considering the spatial variation of ground motion. Hence, this paper takes a multi-span continuous beam bridge as the engineering background and uses the models of evolutionary power spectra of spatially variable seismic ground motions to simulate the time histories of the inconsistent seismic excitation by spectral representation method. After that, the finite element model of multi-span continuous beam bridge is established by

OpenSees and its responses are calculated. Finally, the fragility curves of the bridge considering the spatial variation of ground motions are obtained and compared with the fragility curves under consistent earthquake excitation. The influence of the spatial variation of ground motion on the safety of the bridge is also analyzed.

2. Seismic Fragility Analysis of Bridge

2.1 Method

Structural seismic fragility, which refers to the probability of a structure reaching or exceeding a certain ultimate state (performance level) under the action of ground motion with different intensities, includes structural seismic response analysis and damage analysis. Probabilistic seismic demand analysis (PSDA) studies the statistical relationship between structural seismic demand (S_d) and ground motion intensity index, *IM*, which Cornell *et al.*[21] suggests to satisfy the following relationship:

$$S_d = aIM^b \tag{1}$$

Taking the logarithm of both sides, Eq. (1) becomes:

$$\ln(S_d) = a + b\ln(IM) \tag{2}$$

Fragility curve describes the conditional probability that seismic demand exceeds structural capacity (S_c) under the action of a specific ground motion intensity. The formula of fragility curve is expressed as follows:

$$P_f = P[S_d \geq S_c \mid IM] \tag{3}$$

where, P_f is the probability of the structural failure, S_d is the structural demand, S_c is the structural capability, *IM* is the intensity of ground motion. Peak ground acceleration (PGA) and spectral acceleration (S_a) are usually used as the intensity of ground motion.

In general, the seismic capacity and the seismic demand are both assumed to obey lognormal distribution. In this situation, according to Eq. (3), the probability of structural failure can be represented as:

$$P_f = \Phi[\frac{\ln(S_d / S_c)}{\sqrt{\beta_c^2 + \beta_d^2}}] \tag{4}$$

where Φ is the standard normal distribution function, β_d and β_c are respectively the logarithmic standard deviation of demand and capacity. According to HAZUS-99, when PGA is adopted as the ground motion intensity index,

$$\sqrt{\beta_c^2 + \beta_c^2} = 0.5 \tag{5}$$

2.2 Performance level of multi-span continuous beam bridge

The key of performance-based seismic design is to determine the damage state and the damage index of the structure. This paper divides the damage state into five grades: prefect, slight damage, moderate damage, extensive damage and complete damage. The commonly used vulnerability indexes include Park-Ang index, displacement ductility ratio index and deflection ductility μ_ϕ ratio index. In this paper, the pier adopts curvature ductility ratio to characterize the structural performance and define the damage state:

$$\mu_\phi = \frac{\phi}{\phi_{y1}} \tag{6}$$

where ϕ is the maximum curvature of pier section and ϕ_{y1} is the curvature of the dangerous section of pier longitudinal reinforcement at the first yield. The moment - curvature analysis was carried out on the pier bottom section, as shown in Figure 1.

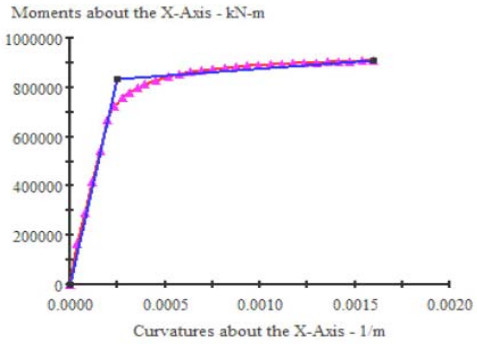

Fig. 1 – The moment-curvature analysis of dangerous sections.

Table 1 – Pier damage states

Damage state	Description of damage state	Damage index
Prefect	There are no obvious cracks in the pier and no yielding of steel reinforcement.	$0 \le \mu_\phi \le \mu_y$
Slight damage	Obvious cracks appeared in the pier column and the outmost steel bar yielded for the first time.	$\mu_y \le \mu_\phi \le \mu_{y1}$
Moderate damage	The surface layer concrete part falls off, the pier produces the non-linear deformation, the pier bottom plastic hinge forms.	$\mu_{y1} \le \mu_\phi \le \mu_{y2}$
Extensive damage	The protective layer of concrete falls off completely, plastic hinge is formed completely, steel bars yield a lot, and concrete cracks in the core area.	$\mu_{y2} \le \mu_\phi \le \mu_{y\max}$
collapse	The core concrete is crushed, the longitudinal bars are broken, the overall strength is lost, and collapse may occur.	$\mu_\phi \ge \mu_{y\max}$

Table 1 presents the damage states of the pier. In Table 1, μ_{y1} is the ratio between the curvature corresponding to the equivalent yield of the longitudinal reinforcement in the dangerous section and the curvature of the longitudinal reinforcement at the first yield, that is, the equivalent yield curvature ductility ratio. μ_{y2} is the ductility ratio of deflection when the compressive strain of concrete reaches 0.0033; $\mu_{y\max}$ is the ratio of curvature ductility when concrete reaches the ultimate compressive strain. The above critical curvature is extracted from Figure 1 and Table 2. According to the above definition, damage index of bridge piers and supports can be determined by Table 2.

Table 2 – Pier damage state and the corresponding damage index

Damage state	Corresponding curvature(1/mm)	Damage index
slight damage	1.937×10^{-7}	1
moderate damage	2.474×10^{-7}	1.25
extensive damage	5.470×10^{-7}	2.77
complete collapse	1.598×10^{-6}	8.10

Figure 2 present the procedure of fragility analysis of multi-span continuous beam bridge considering spatially variable seismic ground motions.

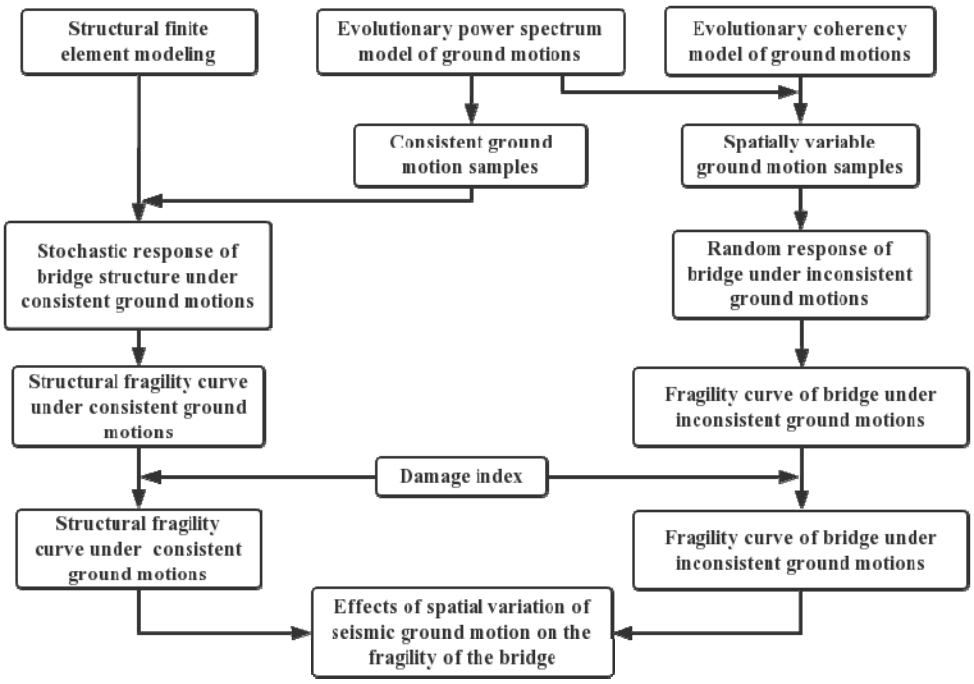

Fig. 2 –The procedure of fragility analysis of multi-span continuous beam bridge considering spatially variable seismic ground motions

3. Finite element model of the bridge and ground motion simulation

3.1 Finite element model

Here a reinforced concrete continuous beam bridge with spans of 84+156×3+84m is studied. The main beam is a single box with concrete C55 . The beam height at the fulcrum of the main span is 11.0m, and the beam height of the straight section of the middle and side span is 6.0m. The height of the beam and the thickness of the bottom plate are designed by quadratic parabola. The bottom structure of the bridge is gravity type circular end-shaped pier, which is made of concrete C35 with a height of 36m. HRB335 reinforcement is used for both longitudinal reinforcement and stirrup. The reinforcement ratio of longitudinal reinforcement is 1.630%, the volume ratio of stirrup is 0.52%, the diameter of longitudinal reinforcement is 35mm, the diameter of stirrup is 12mm, and the thickness of protective layer is 7cm.The seismic fortification intensity is 7 degrees, and the designed basic seismic acceleration is 0.15g.

In this paper, the OpenSees program is used to build a full bridge nonlinear finite element model. The investigation of a large number of actual seismic damage shows that the main beams of most continuous girder Bridges basically maintain linear elastic state under earthquake action, so this paper adopts linear elastic beam-column element to simulate the superstructure and elastoplastic fiber element to simulate the piers. In the elastic-plastic element of pier, considering the constraint effect of stirrup, the concrete model adopts Kent- scott-park model without considering the tensile effect, and USES Concrete01 simulation in openSees. Steel reinforcement adopts hardened elastic-plastic model, which is simulated by Steel01 and the support is simulated by zero - length element. The circular end-shaped section of the pier is divided into two parts: the two semi-circular sections of the protective layer of concrete are evenly divided into 12 parts, the core area of concrete is evenly divided into 12 parts, and the radial section is evenly divided into 6 parts.The

rectangular section of the protective layer of concrete is evenly divided into 16 parts, the core area of concrete is evenly divided into 15×15 parts, and the longitudinal stress reinforcement is evenly distributed on the boundary between the protective layer and the core concrete. The pier bottom is consolidated without considering the interaction between pile and soil. The details of the finite element model of the bridge is shown by Figure 3~5.

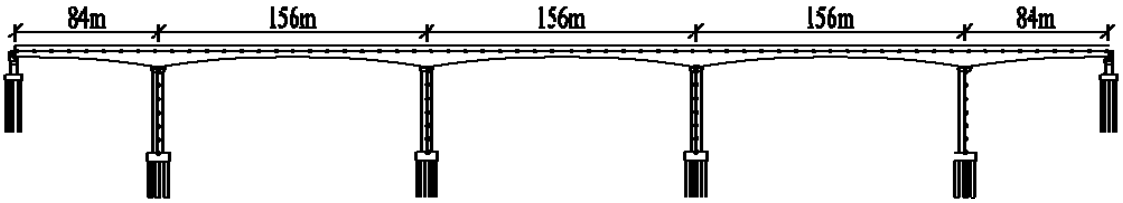

Fig. 3 – Finite element model of continuous beam bridge

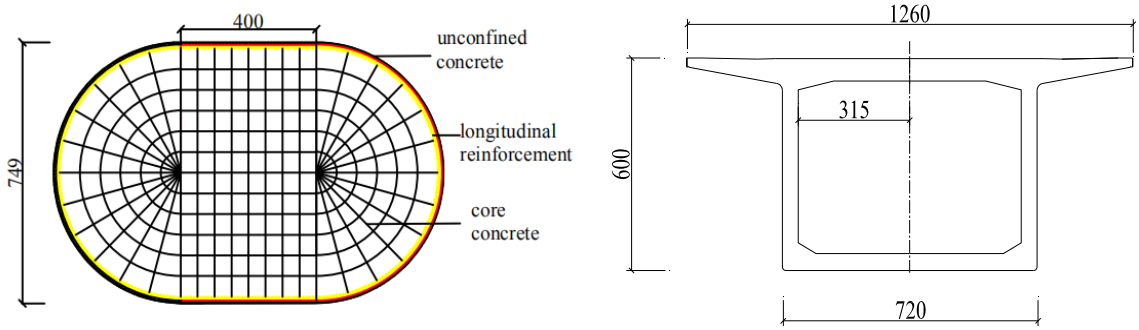

Fig. 4 – Pier fiber section and main beam cross section

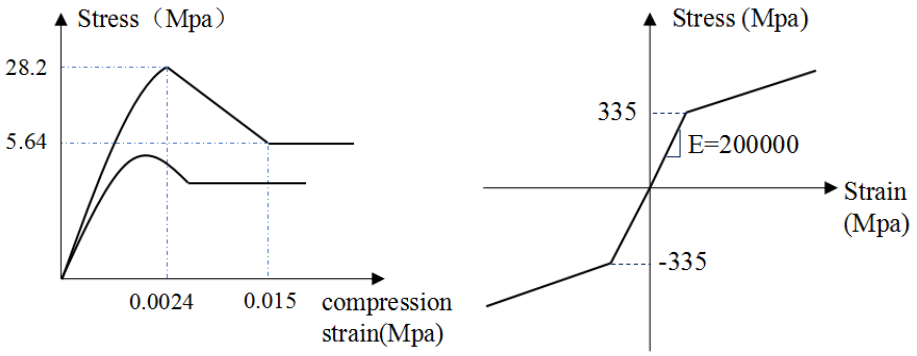

Fig. 5 – Concrete and steel constitutive models

When the model is completed, the modal analysis is carried out. The period of the first-order mode is T=1.0715s, which is similar to that of similar span bridges of the same type, to verify the correctness of the model.

3.2 Ground motion simulation

In this paper, peak ground acceleration (PGA) is selected as the indicator of ground motion intensity, and the evolutionary power spectrum mode of seismic ground motion is used to simulate artificial ground motion time history. 20 groups of seismic ground motion time histories are generated. The average range of peak acceleration (PGA) is from 0.1g to 1.5g (see Table 3), with a total of 4,200 seismic waves. Fig. 6 shows

typical seismic time history samples of PGA at 0.1, 0.5, 1.0 and 1.5g. Some typical ground motion time histories are shown in Figure 6.

Table 3 – Value of peak ground acceleration

Number	PGA	lnPGA	Number	PGA	lnPGA
1	0.1	-2.30	9	0.9	-0.11
2	0.2	-1.61	10	1.0	0
3	0.3	-1.20	11	1.1	0.10
4	0.4	-0.92	12	1.2	0.18
5	0.5	-0.69	13	1.3	0.26
6	0.6	-0.51	14	1.4	0.34
7	0.7	-0.36	15	1.5	0.41
8	0.8	-0.22			

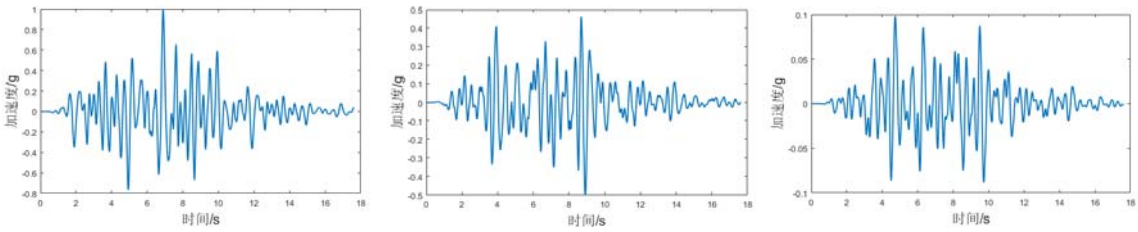

Fig. 6 – Typical seismic time history

4. Fragility analysis of the continuous beam bridge

4.1 Seismic response analysis of continuous girder Bridges

Under these ground motion input of the finite element model of the continuous beam bridge, No. 4 pier bearing adopts fixed bearing, that is, the nonlinear structural response of No. 4 pier and the main beam bearing is extracted when the PGAs are 0.1g, 0.3g and 0.5g respectively, as shown in Figures 7~10.

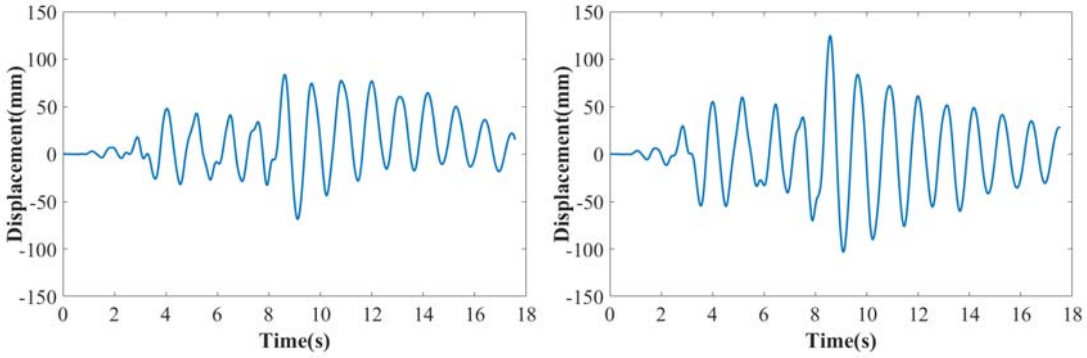

(a). Inconsistent ground motion input (b). Consistent ground motion input

Fig. 7 – Displacement of the top section of No.4 pier shifted along the bridge when the PGA is 0.3g

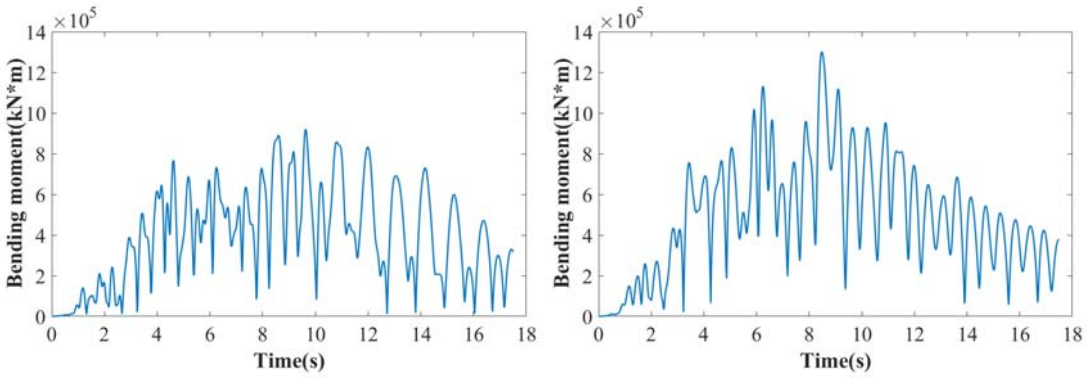

(a). Inconsistent ground motion input (b). Consistent ground motion input

Fig. 8 – Bending moment of the bottom section of No.4 pier when the PGA is 0.3g

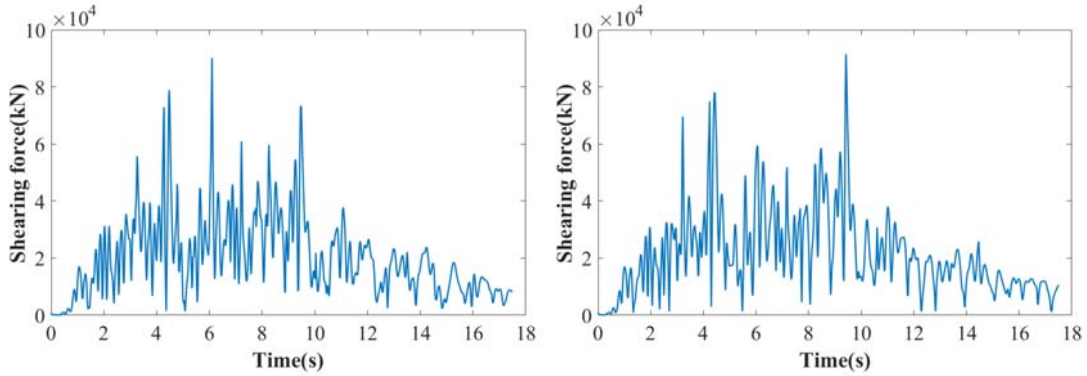

(a). Inconsistent ground motion input (b). Consistent ground motion input

Fig. 9 – Shearing force of the bottom section of No.4 pier when the PGA is 0.3g

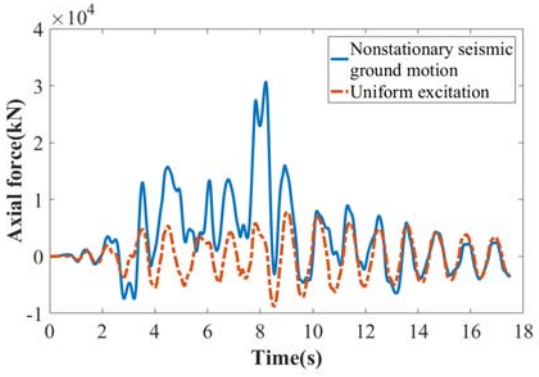

Fig.10 –Time history samples of the axial force of the main beam when the PGAs are 0.3g

4.2 Fragility curve calculation

The seismic fragility curves of continuous beam bridge is analyzed based on the calculation result of the response of the finite element model. The simulated 20 groups of ground motion samples are loaded into the finite element model to calculate the responses under the inconstant and constituent seismic excitation. The maximum curvature ductility ratio of the corresponding pier is obtained. Regression processing is carried out according to the steps described in section 2 to obtain the relationship between structural response and peak acceleration, as shown in the Figure 11.

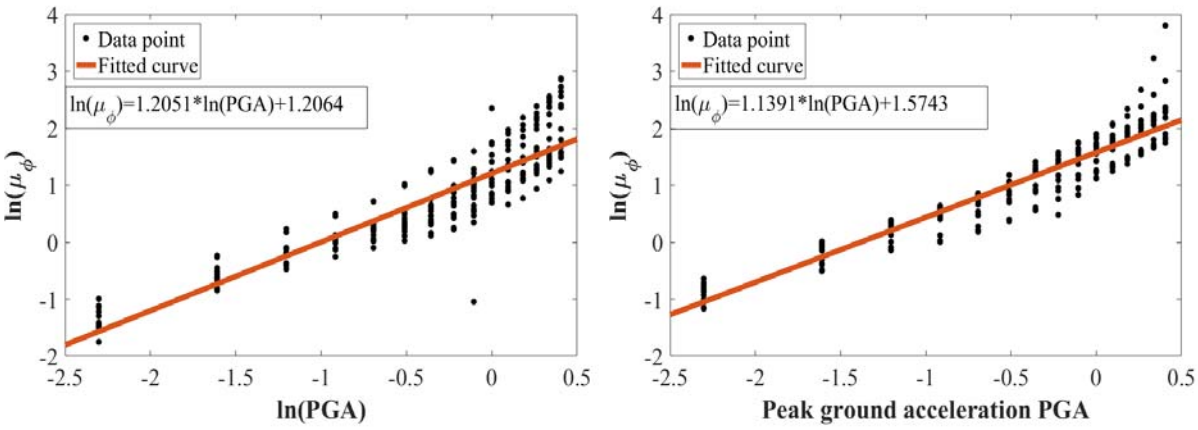

(a). Inconsistent (b). Consistent

Fig. 11 – Regression analysis of the seismic demand response of the pier under the inconsistent and consistent ground motions

As shown in Figure 11, the fitting regression equation under the consistent ground motions is：

$$\ln(\mu_\phi) = 1.1391 \cdot \ln(\mathrm{PGA}) + 1.5743 \tag{7}$$

and that under the inconsistent ground motions is:

$$\ln(\mu_\phi) = 1.2051 \cdot \ln(\mathrm{PGA}) + 1.2064 \tag{8}$$

Under the consistent excitation, the expressions of the fragility curves of the slight, moderate, extensive and complete damages are：

$$\begin{aligned} P_f &= \Phi\left[\frac{1.1391\cdot\ln(\mathrm{PGA})+1.5743-\ln(1.0)}{0.5}\right] \\ P_f &= \Phi\left[\frac{1.1391\cdot\ln(\mathrm{PGA})+1.5743-\ln(1.25)}{0.5}\right] \\ P_f &= \Phi\left[\frac{1.1391\cdot\ln(\mathrm{PGA})+1.5743-\ln(2.77)}{0.5}\right] \\ P_f &= \Phi\left[\frac{1.1391\cdot\ln(\mathrm{PGA})+1.5743-\ln(8.10)}{0.5}\right] \end{aligned} \tag{9}$$

Under the inconsistent excitation, the expressions of the corresponding fragility curves are：

$$\begin{aligned} P_f &= \Phi\left[\frac{1.2051\cdot\ln(\mathrm{PGA})+1.2064-\ln(1.0)}{0.5}\right] \\ P_f &= \Phi\left[\frac{1.2051\cdot\ln(\mathrm{PGA})+1.2064-\ln(1.25)}{0.5}\right] \\ P_f &= \Phi\left[\frac{1.2051\cdot\ln(\mathrm{PGA})+1.2064-\ln(2.77)}{0.5}\right] \\ P_f &= \Phi\left[\frac{1.2051\cdot\ln(\mathrm{PGA})+1.2064-\ln(8.10)}{0.5}\right] \end{aligned} \tag{10}$$

The fragility curves are given in Figure 19. As shown by Figures 19~20, under the inconsistent and the consistent seismic ground motions, the pier won't be almost damaged when the PGA is 0.15g. When the

failure probability of serious damage exceeds 50%, the corresponding PGA exceeds 0.5g, and when the failure probability of complete collapse exceeds 50%, the corresponding PGA exceeds 1.4g, indicating that the structure has sufficient seismic resistance and meets the seismic design specifications of Bridges in China. The PGA corresponding to the probability of minor damage over 50% is around 0.3g, indicating that the bridge is vulnerable.

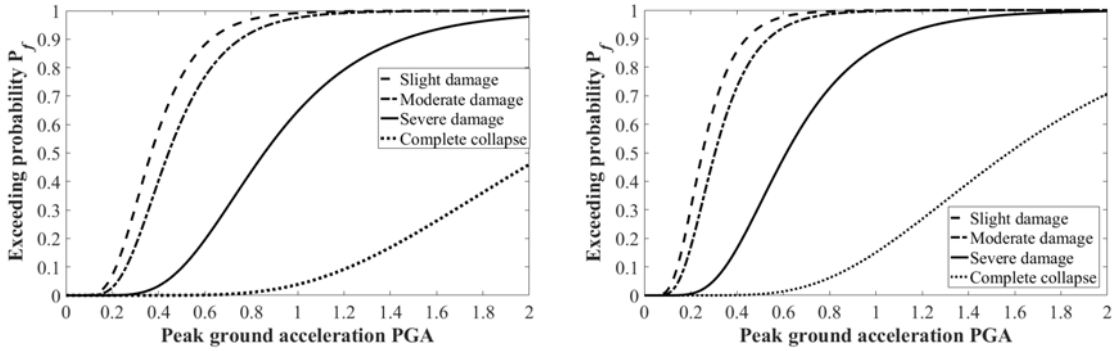

(a). Inconsistent (b). Consistent

Fig. 12 – The fragility curves of the bridge under the inconsistent and consistent ground motions

The fragility curve of the bridge pier in Figure 12 is sorted out, and the four damage degrees of slight damage, moderate damage, extensive damage and complete collapse are distinguished. The vulnerability curve of the bridge pier under the action of ground motion and consistent excitation is made under each damage degree, as shown in Figure 13.

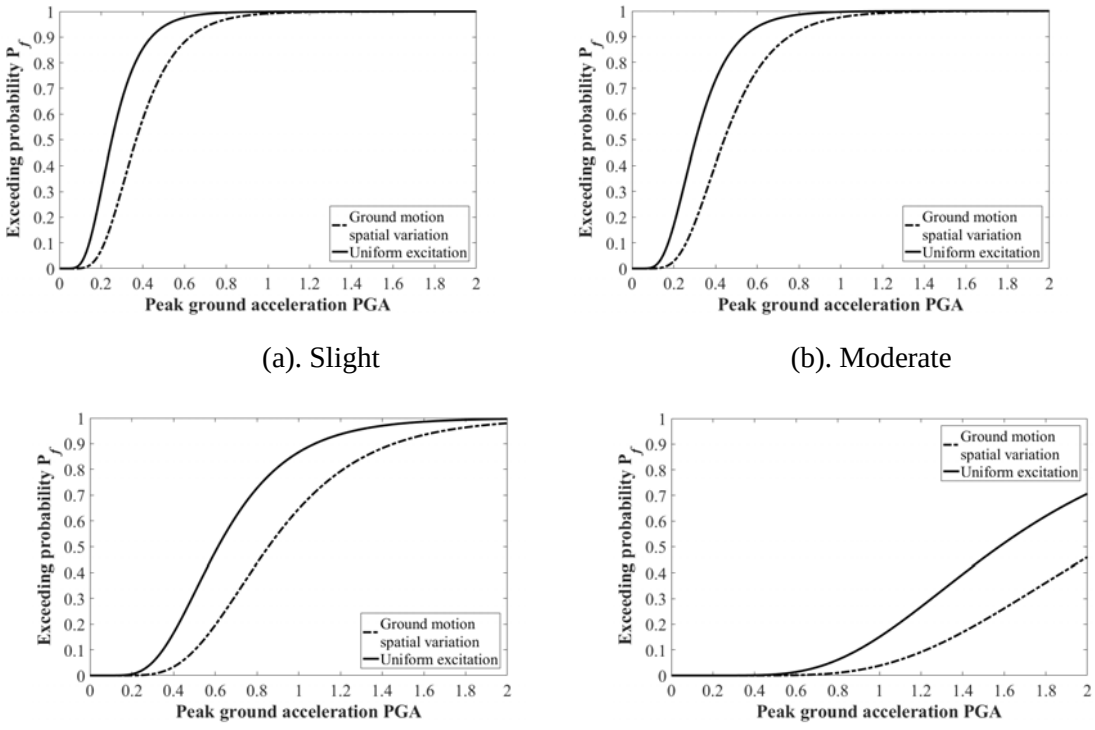

(a). Slight (b). Moderate

(c). Extensive (d). Complete

Fig. 13– The fragility curves of the bridge for different damage states

4.3 Effect of seismic spatial variation on the fragility curve

Figure 21 indicates that the bridge is more vulnerable under consistent seismic excitation. By taking the inverse function of equations (7) and (8), it can be obtained as:

$$\mathrm{PGA}_1 = e^{\left(\frac{\ln \mu_\phi - 1.2064}{1.2051}\right)}, \quad \mathrm{PGA}_2 = e^{\left(\frac{\ln \mu_\phi - 1.5743}{1.1391}\right)} \tag{11}$$

where PGA_1 and PGA_2 respectively represent the peak acceleration of ground motion under inconsistent and consistent seismic ground motions. The corresponding values of PGA_1 and PGA_2 are calculated by taking the same value of $\ln \mu_\phi$. According to the regression result, the relationship between the PGA_1 and PGA_2 is:

$$\mathrm{PGA}_2 = 0.75 \cdot \mathrm{PGA}_1 - 0.02 \tag{12}$$

as shown by Figure 14.

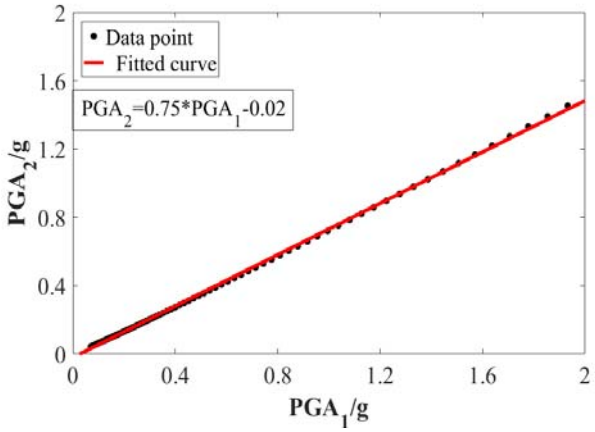

Fig. 14 – The relationship between the PGAs of the inconsistent and consistent seismic ground motions under the same damage degree of the bridge

5. Conclusion

In this paper, the fragility curves of a multi-span continuous beam bridge under inconsistent seismic ground motions are calculated and its vulnerability curve are calculated. The effect of the spatial variation of seismic ground motions is also discussed. The conclusions include:

(1). The finite element model of a multi-span continuous beam bridge is carried out and the time history samples of spatially variable seismic ground motions are simulated by the spectral representation method. The responses of the bridge under inconsistent and constituent ground motions are also calculated. Using the curvature ductility ratio as the damage index, the fragility curves of the multi-span continuous beam bridge under inconsistent and constituent ground motions are calculated for different damage states.

(2). Comparison between the fragility curves of the bridges under the inconsistent and consistent ground motions indicates the multi-span continuous beam bridge is more vulnerable under consistent ground motions.

6. References

This research was supported by National Natural Science Foundation of China (51408526 & 51678465) and Scientific and Technological Research Projects of Colleges and Universities in Hebei Province (BJ2019030).

7. References

[1] Lv D, Yu X. Theoretical study of probabilistic seismic risk assessment based on analytical functions of seismic fragility[J]. *Journal of Buliding Structures*, 2015, 34(10): 41-48.

[2] Billah A H M, Alam M S. Seismic fragility assessment of highway bridges: a state-of-the-art review [J]. *Structure and Infrastructure Engineering*, 2015, 11(6): 804-832.

[3] Basöz N I, Kiremidjian A S. Statistical Analysis of Bridge Damage Data from the 1994 Northridge, CA, Earthquake[R]. *Technical Report Nceer*, 1997.

[4] Basöz, Nesrin I, Kiremidjian A S . Evaluation of bridge damage data from the Loma, Prieta and Northridge, California earthquakes[R]. *Technical Report Mceer*, 1998.

[5] Shinozuka M, Feng M Q, Lee J, et al. Statistical Analysis of Fragility Curves[J]. *Journal of Engineering Mechanics*, 2000, 126(12):1224-1231.

[6] Shinozuka M, Saxena V, Deodatis G. Effect of spatial variability of ground motion on bridge fragility curves[C]. *Proceedings of the 8th ASCE Specialty Conference on Probabilistic Mechanics and Structural Reliability*, 2000:1-6.

[7] Monti G, Nisticò, Nicola. Simple Probability-Based Assessment of Bridges under Scenario Earthquakes[J]. *Journal of Bridge Engineering*, 2002, 7(2):104-114.

[8] Karim K R, Yamazaki F. A simplified method of constructing fragility curves for highway bridges[J]. *Earthquake Engineering & Structural Dynamics*, 2003, 32(10):1603-1626.

[9] Elnashait A S, Borzi B, Viachost S. Deformation-based vulnerability functions for RC bridges[J]. *Structural Engineering & Mechanics*, 2004, 17(2).

[10] Lehman D, Moehle J, Mahin S, *et al.*. Experimental Evaluation of the Seismic Performance of Reinforced Concrete Bridge Columns[J]. *Journal of Structural Engineering*, 2004, 130(6):869-879.

[11] Jeong S H, Elnashai A S. Probabilistic fragility analysis parameterized by fundamental response quantities[J]. *Engineering Structures*, 2007, 29(6):1238-1251.

[12] Liao G, Chen B, Chen S. Response Analysis of the High-piers and Long-span Rigid Frame Bridge Subjected to Varying Spatial Seismic Excitation[J]. *Journal of Sichuan University*, 2011,43(5):27-44.

[13] Li J, Yang Q, Liu Y. Fragility analysis of long span continuous rigid frame bridge under multi-support excitations[J]. *Journal of Vibration and Shock*, 2013,32(5):75-80.

[14] Han X, Li X, Xiang B, *et al.*. Analysis of Seismic Fragility of High Speed Railway Continuous Beam Bridge Based on IDA Method[J]. *Journal of Highway and Transportation Research and Development*, 2016,33(2):54-59.

[15] Li C, Hao H. Seismic fragility analysis of reinforced concrete bridges with chloride induced corrosion subjected to spatially varying ground motions [J]. *International Journal of Structural Stability and Dynamics*, 2016,16(05):1550010.

[16] Li L, Li H, Xu K, *et al.*. Bridge Seismic Fragility Analysis Considering Random Variable Correlations[J]. *Journal of Hunan University*, 2017,44(7):118-127.

[17] Liu C, Ren W. Vulnerability analysis of offshore isolation bridge based on Monte Carlo sampling[J]. *Journal of natural disasters*, 2017,26(1):108-117.

[18] Kang R, Zheng K, Li X, *et al.*. Effect of Ground Motion Spatial Variations on Pounding Response of High-Pier Railway Bridge[J]. *Journal of Southwest Jiaotong University*, 2018,53(3): 483-499.

[19] Guideline for Seismic Design of Highway Bridges[M]. *China Communications Press*, 2008.

[20] Der Kureghian A, Neuenhofer A. Response spectrum method for mulit-support seismic excitations[J]. *Earthquake Engineering and Structural Dynamics*, 1992,21(8): 713-740.

[21] Cornell C A, Jalayer F, Hamburger R O, *et al.*. Probabilistic Basis for 2000 SAC Federal Emergency Management Agency Steel Moment Frame Guidelines[J]. *Journal of Structural Engineering*, 2002, 128(4): 526-533.

